Supporting information for

Maximizing Active Site Utilization in Carbocatalysts for High-Performance Oxygen Reduction Reactions and Zinc-Air Battery-Powered Capacitive Deionization

Xiaofeng Mou[1], Jiale Zhang[1], Bin Zhao[1], Yanli Dong[1], Huimin Liu[1], Jiaxu Liang[2]*, Xiaoyu Xin[1], Yusuke Asakura[3], Shuaihua Zhang[1]*, Zhichang Xiao[1]* and Yusuke Yamauchi[3, 4, 5]*

[1] Department of Chemistry, College of Science, Hebei Agricultural University, Baoding 071001, People's Republic of China.

[2] Max Planck Institute for Polymer Research, Ackermannweg 10, 55128 Mainz, Germany

[3] Department of Materials Process Engineering, Graduate School of Engineering, Nagoya University, Nagoya 464-8603, Japan

[4] Australian Institute for Bioengineering and Nanotechnology (AIBN), The University of Queensland, Brisbane, QLD 4072, Australia

5 Department of Chemical and Biomolecular Engineering, Yonsei University, 50 Yonsei-ro, Seodaemun-gu, Seoul 03722, South Korea

*Corresponding authors:

E-mail: liangjiaxu@mpip-mainz.mpg.de (J. Liang); zhangshuaihua@hebau.edu.cn (S. Zhang); xiaozhichangcnu@sina.cn (Z. Xiao); y.yamauchi@uq.edu.au (Y. Yamauchi).

Experimental Section

1.1 Materials and Reagents

Indole (C_8H_7N, 99%) was purchased from MACKLIN. Iron (III) chloride ($FeCl_3$, AR) was sourced from Shanghai Boer Chemical Reagents CO., Ltd. Zinc chloride ($ZnCl_2$, AR, ≥98%) was acquired from Shanghai Aladdin Biochemical Technology Co., Ltd. Sodium chloride (NaCl, ≥99.5%) was obtained from Tianjin Fengchuan Chemical Reagent Technology Co., Ltd. 20 wt% Pt/C was purchased from MERYER. 1,2-Dichloroethane (AR) and Ethanol 95% (EtOH, AR) were bought from Tianjin Damao Chemicals Reagent Factory. Dimethoxymethane ($C_3H_{11}O_2$, 98%) and Nafion solution (5 wt%) were supplied by Alfa Aesar. All chemicals were used as received without further purification.

1.2 Material Characterization

The morphology of the catalyst was investigated using scanning electron microscope (SEM, Hitachi, Japan) and transmission electron microscope (TEM, FEI, USA). The phase composition of the samples was analyzed using an X-ray diffraction spectrometer (XRD, Rigaku, Japan). The defective structure of the catalyst structure was characterized by Raman spectroscopy (Raman, Renishaw, UK) and electron paramagnetic resonance (EPR, Bruker A300 X). The chemical composition of the materials was analyzed using X-ray photoelectron spectroscopy (XPS, Thermo Fisher Scientific). The specific surface area and pore size distribution of the catalyst were determined using an automatic micropore surface area and porosity analyzer (Micromeritics Instrument Corp., USA).

1.3 Electrochemical measurements

Preparation of catalyst slurry: 2.6 mg of finely grounded sample powder was mixed with 300 μL of anhydrous ethanol, 200 μL of deionized water, and sonicated to disperse uniformly before adding 20 μL of Nafion solution (5 wt%). The mixture was sonicated for one hour to obtain a uniform catalyst slurry. All samples and commercial 20 wt% Pt/C were prepared in the same manner.

Preparation of working electrodes: Two types of working electrodes, including RDE and RRDE, were used during electrochemical testing. To prepare the electrodes, RDE

and RRDE were polished with alumina polishing powder of various grades, and then ultrasonically cleaned several times with deionized water. 7 μL and 10 μL of the prepared catalyst slurry were pipetted onto the glassy carbon surface of the RDE and RRDE, respectively, and allowed to dry naturally overnight. All samples, including the commercial 20 wt% Pt/C, were prepared in the same manner for use as working electrodes.

Electrochemical testing: All electrocatalytic performance tests were conducted using a CHI 760E electrochemical workstation and a rotating ring-disk electrode apparatus. The measurement employed a three-electrode system, including the prepared RDE and RRDE served as the working electrodes, Ag/AgCl as the reference electrode, and a graphite rod as the counter electrode. 0.1 M KOH aqueous solution was used as the electrolyte. Before testing, the solution was purged with nitrogen or oxygen for 30 minutes to ensure gas saturation, with continuous gas flow maintained throughout the testing process. Initially, multiple cyclic voltammetry (CV) tests were performed to fully activate the electrodes.

The cyclic voltammetry tests were obtained from -1 V to 0.1 V at a scan rate of 20 mV s^{-1}. Subsequently, linear sweep voltammetry (LSV) tests were conducted on the RDE at 1600 rpm to obtain key performance evaluation data such as half-wave potential ($E_{1/2}$), and kinetic current density. By varying the RDE rotation speed from 2500 to 400 rpm in descending order, a series of LSV curves at different speeds were obtained. The electron transfer number (n) and kinetic current density (J_k) were then determined using the Koutecky-Levich (K-L) equation:

$$\frac{1}{J}=\frac{1}{J_L}+\frac{1}{J_k}=\frac{1}{B\omega^{1/2}}+\frac{1}{J_k} \quad (1)$$

$$B=0.62nFC_0(D_0)^{2/3}\nu^{-1/6} \quad (2)$$

$$J_k=nFkC_0 \quad (3)$$

where J represents the actual measured current density, J_L the limiting diffusion current density, J_k the limiting kinetic current density, ω the electrode rotation speed (rpm), F

the Faraday constant (96485 C mol^{-1}), n the number of electrons transferred per oxygen molecule, k the electron transfer rate constant, C_0 the volume concentration of oxygen (1.2×10^{6} mol cm^{-3} in 0.1 M KOH electrolyte), D_0 the diffusion coefficient of oxygen (1.9×10^{-5} cm^2 s^{-1} in 0.1 M KOH electrolyte), and υ the kinetic viscosity of the electrolyte (0.01 cm^2 s^{-1}).

Furthermore, the electron transfer number (n) and H_2O_2 yield were also determined using the RRDE. When the RRDE served as the working electrode, H_2O_2 produced on the glassy carbon surface was collected by the platinum ring under centrifugal force at rotation speed of 1600 rpm. By applying a reverse voltage to the platinum ring, H_2O_2 was oxidized back to O_2, and the current density generated by the platinum ring was recorded to calculate the amount of O_2 reduced to H_2O_2. The n and H_2O_2 yield were further calculated using the following equations:

$$HO_2^-(\%)=200\frac{I_r/N}{I_d+I_r/N} \quad (4)$$

$$n=4\frac{I_d}{I_d+I_r/N} \quad (5)$$

where n represents the electron transfer number, I_r the ring current obtained from RRDE measurement, I_d the disk current, and N the collection efficiency of the platinum ring (0.358 in our instrument).

1.4 Aqueous Zinc-Air Battery (ZAB)

Polished zinc plates were used as the anode, and carbon paper loaded with the catalyst served as the cathode, with a mixed electrolyte of 6 M KOH and 0.2 M zinc acetate aqueous solution. The catalyst slurry was prepared by dispersing 1 mg of the catalyst (NPC-Zn or Pt/C) in a mixture of 300 μL anhydrous ethanol, 200 μL distilled water, and 20 μL Nafion (5 wt%) solution, followed by 30 minutes of ultrasonic treatment. Additionally, a slurry of 0.5 mg Pt/C and 0.5 mg IrO_2 was prepared using the same method. All electrochemical tests were conducted at ambient conditions, with LSV polarization curves obtained using a CHI 760E electrochemical workstation at a scan rate of 5 mV s^{-1}. Galvanostatic charge-discharge cycling tests were performed on a CT2001A testing system at a current density of 5 mA cm^{-2}.

The specific capacity was calculated using the following formula:

$$C\ (mAh/g)=\frac{I\times t}{m_{Zn}} \quad (6)$$

where I represents the test current, t the test duration, and m_{Zn} the mass of consumed zinc.

The Columbic efficiency (CE) was calculated according to the following equation:

$$CE=\frac{C_d}{C_c+m_{Zn}\times 820/N}\times 100\% \quad (7)$$

where C_d is the discharge capacity (mAh), C_c is the charge capacity (mAh), m_{Zn} is the mass loss of Zn during the tests (g), and N is the number of cycles.

1.5 Capacitive deionization (CDI) performance

CDI performance testing was conducted using a continuous cycling system, consisting of a pair of working electrodes, anion and cation exchange membranes, a peristaltic pump and a direct-current power supply. The working electrodes were prepared by weighing a mixture of NPC-Zn, carbon black, and PVDF binder with a mass ratio of 8:1:1. After thoroughly grinding, the mixture was spread onto graphite paper (2.5 cm ×2.5 cm). The mixture was vacuum-dried at 60 ℃ for 12 hours.

During CDI testing, a REX DDSJ-308F ion conductivity meter was used to monitor and measure changes in the concentration of NaCl solution exiting the CDI device under different concentrations and voltages in real-time. The volume of the NaCl solution was 32 mL, with a flow rate of 30 mL min^{-1}. The salt adsorption capacity (SAC, mg g^{-1}) within t minutes was calculated using the following equation:

$$SAC=\frac{(C_0-C_t)\times V_S}{m} \quad (8)$$

where C_0 and C_t represent the NaCl concentration (mg L^{-1}) at the initial stage and at t minutes, respectively; V_s represents the volume of the solution (L); m represents the total mass of NPC-Zn on the working electrode (g).

Finally, the assembled ZAB was used to power the CDI device under the same conditions to test its performance.

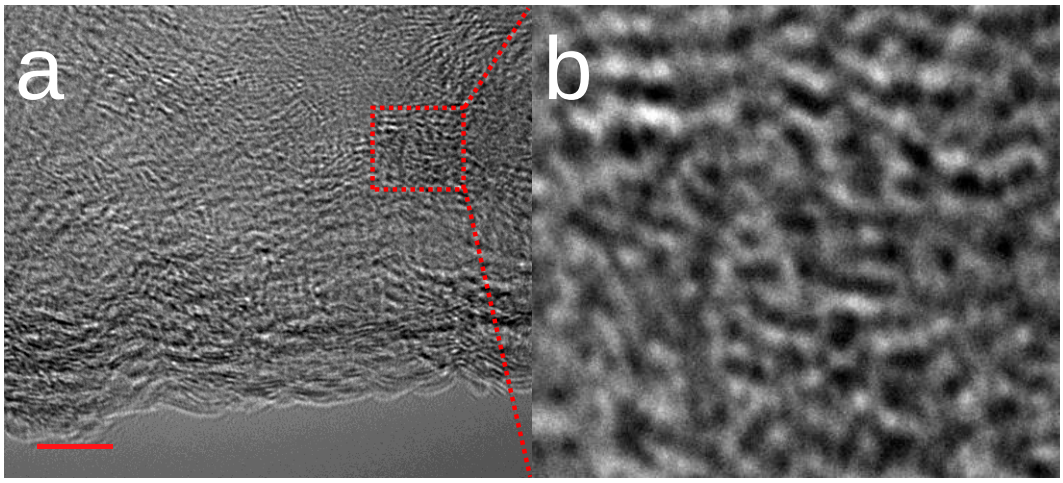

Figure S1. (a) Aberration-corrected TEM image of NPC-Zn; (b) Magnification of the marked areas in (a).

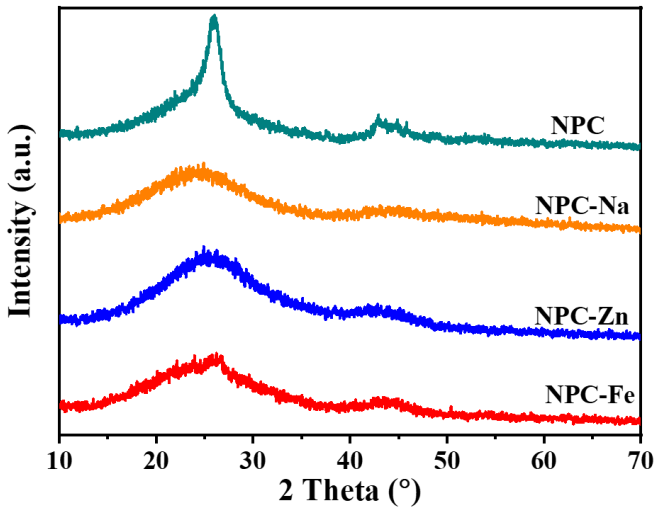

Figure S2. XRD patterns of NPC, NPC-Na, NPC-Zn, NPC-Fe.

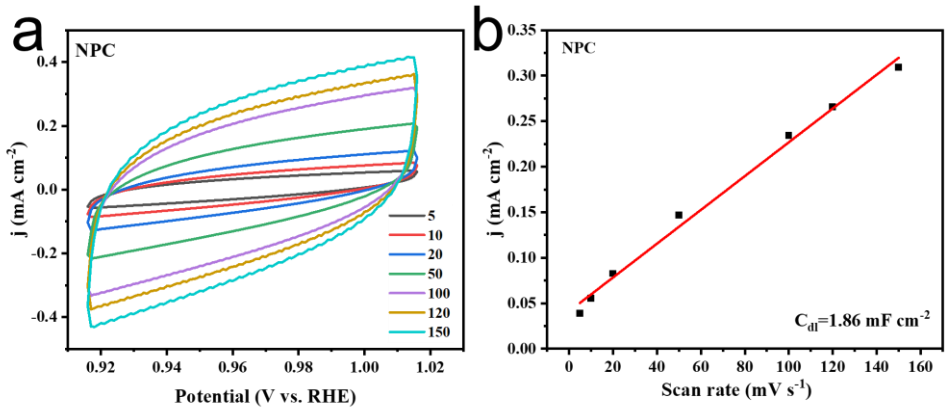

Figure S3. CV curves at different scan rates of NPC and the corresponding current densities at 0.97 V vs. RHE plotted against scan rates; the calculated C_{dl} value is shown in inset.

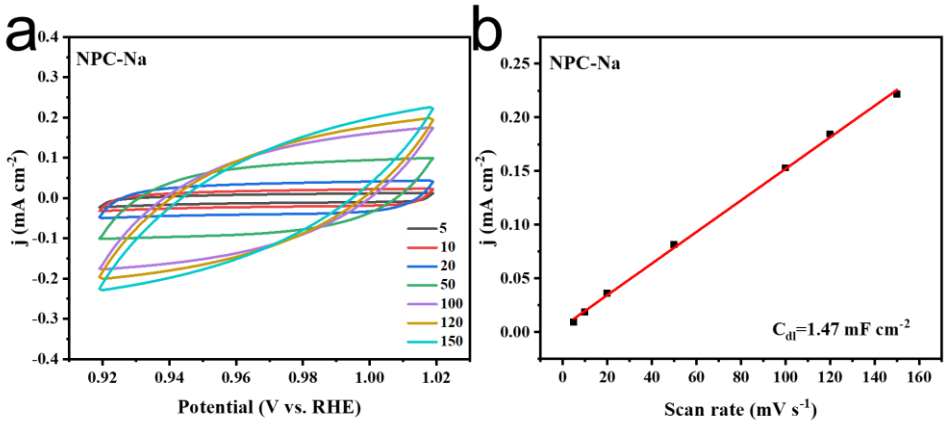

Figure S4. CV curves at different scan rates of NPC-Na and the corresponding current densities at 0.97 V vs. RHE plotted against scan rates; the calculated C_{dl} value is shown in inset.

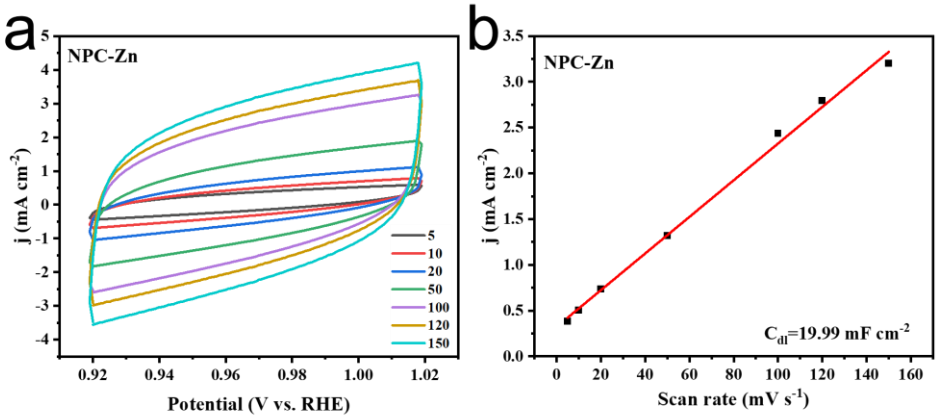

Figure S5. CV curves at different scan rates of NPC-Zn and the corresponding current densities at 0.97 V vs. RHE plotted against scan rates; the calculated C_{dl} value is shown in inset.

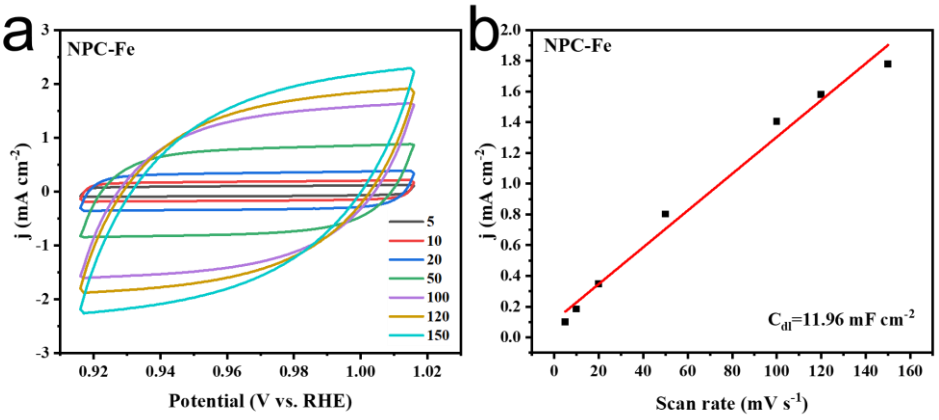

Figure S6. CV curves at different scan rates of NPC-Fe and the corresponding current densities at 0.97 V vs. RHE plotted against scan rates; the calculated C_{dl} value is shown in inset.

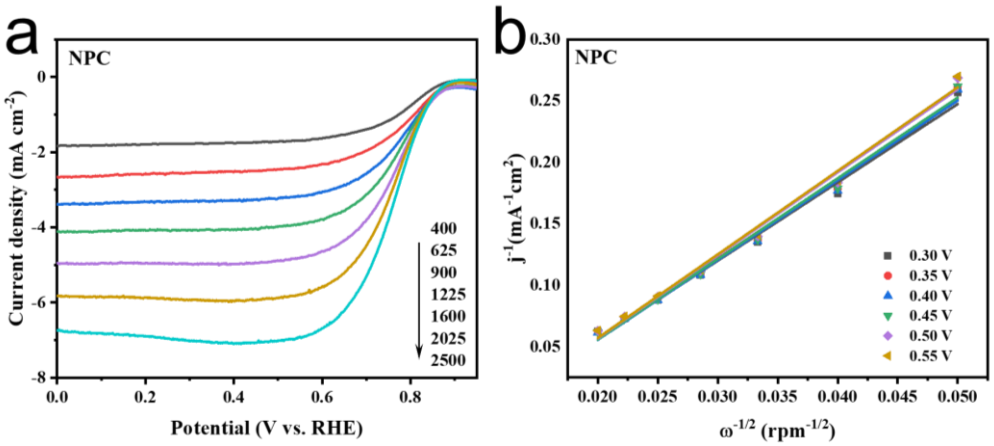

Figure S7. (a) LSVs curves of NPC at different rotating speeds and (b) the corresponding K-L plots at different potentials.

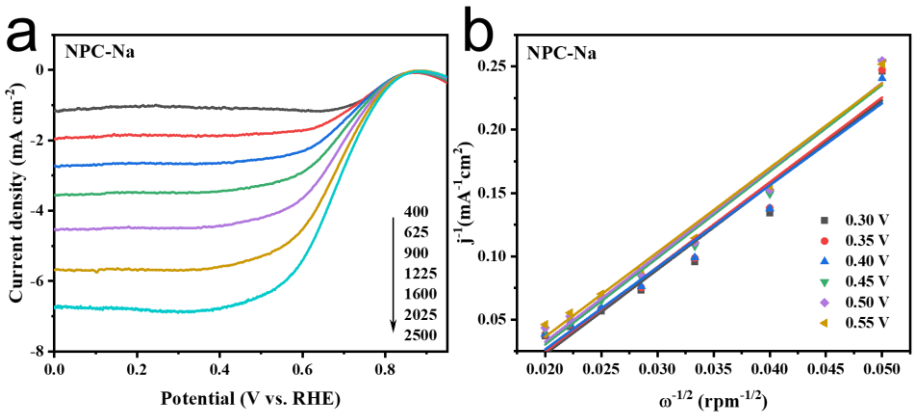

Figure S8. (a) LSVs curves of NPC-Na at different rotating speeds and (b) the corresponding K-L plots at different potentials.

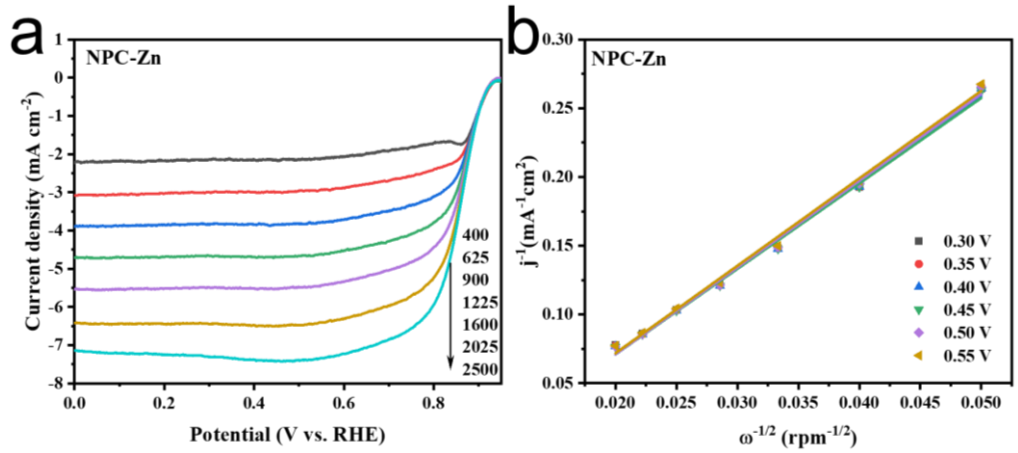

Figure S9. (a) LSVs curves of NPC-Zn at different rotating speeds and (b) the corresponding K-L plots at different potentials.

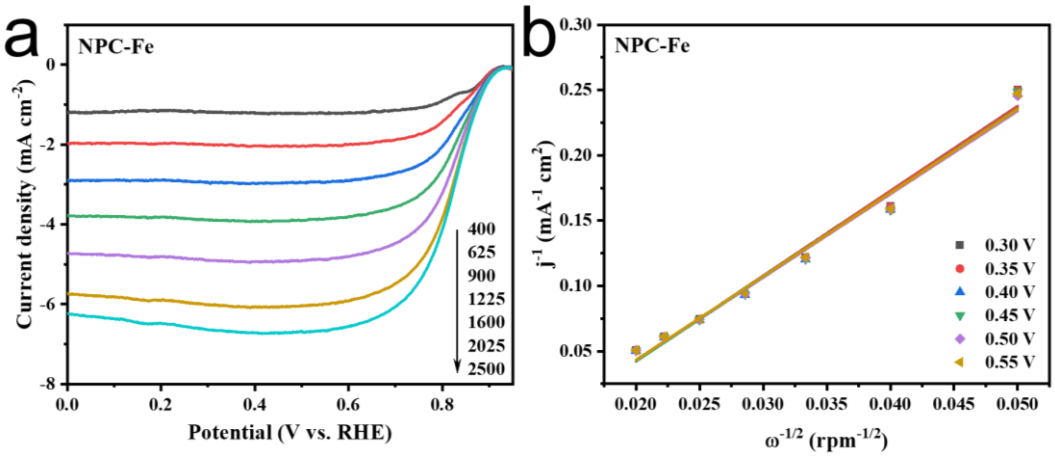

Figure S10. (a) LSVs curves of NPC-Fe at different rotating speeds and (b) the corresponding K-L plots at different potentials.

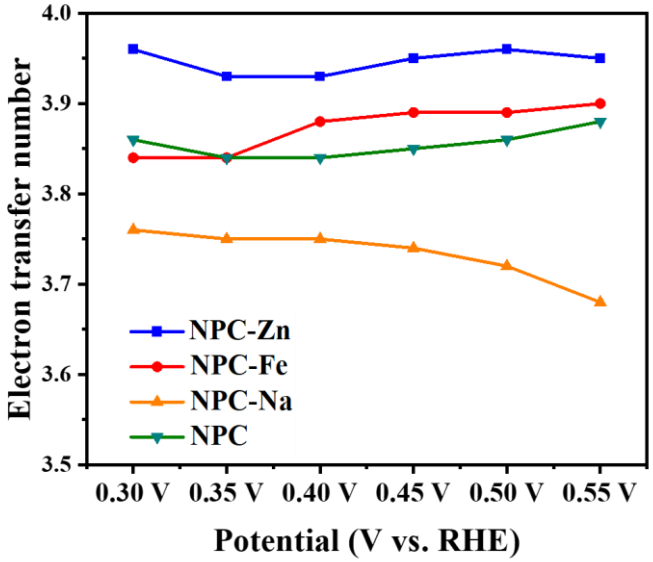

Figure S11. The electron transfer numbers of all the samples in this work between 0.30 V and 0.55 V vs. RHE.

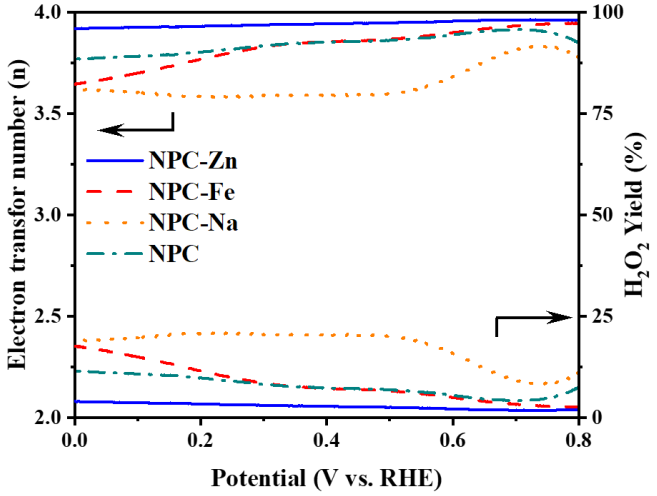

Figure S12. H_2O_2 yield and electron transfer number of all the samples in this work.

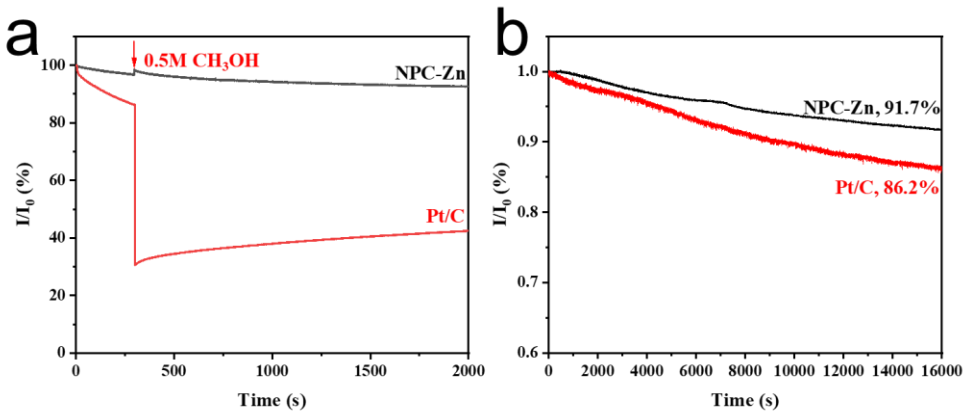

Figure S13. (a) Methanol-tolerance evaluation and (b) the stability of NPC-Zn tested by the current-time chronoamperometric responses at 0.6 V vs. RHE in oxygen-saturated 0.1 M KOH solution.

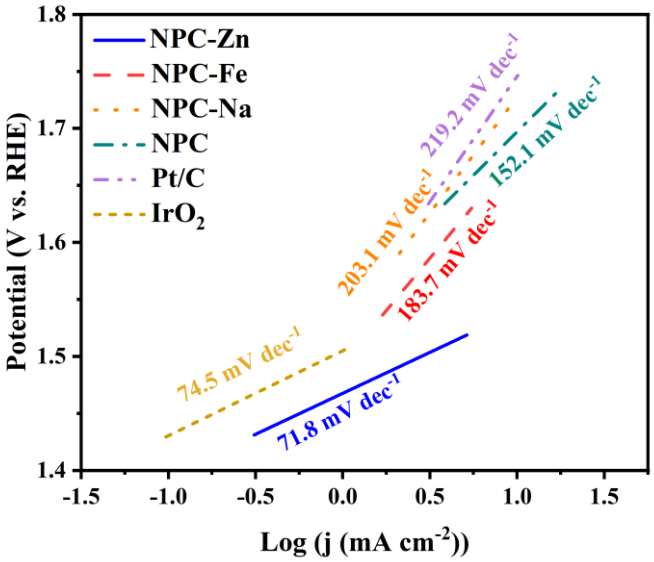

Figure S14. Tafel plots of NPC, NPC-Na, NPC-Zn, NPC-Fe, Pt/C and IrO_2 corresponding to the LSV curves in Figure 3f.

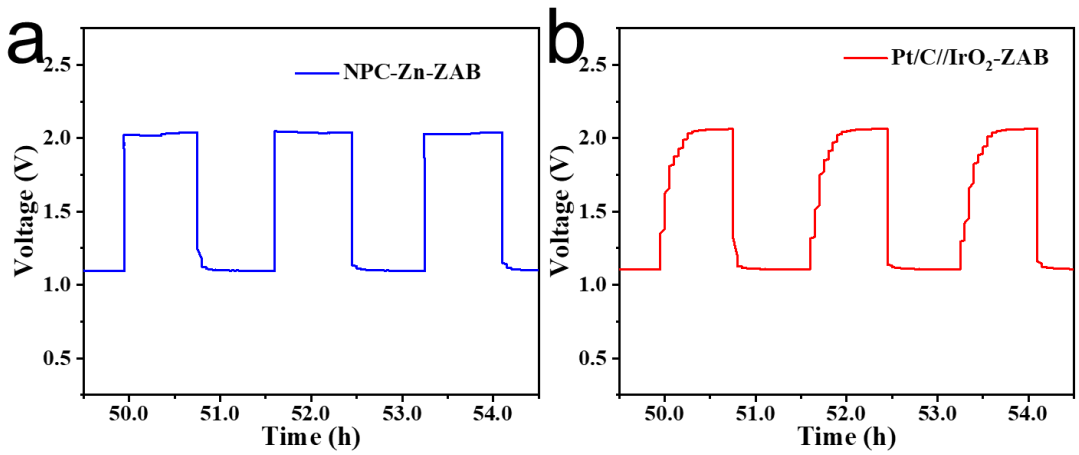

Figure S15. (a) Galvanostatic discharge/charge curves of NPC-Zn-ZAB at 5 mA cm^{-2} for 1.6 h per cycle (0.85 h charge and 0.75 h discharge). Considering m_{Zn} is 0.14825 g, discharge capacity (C_d) is 3.75 mAh, and charge capacity (C_c) is 4.25 mAh, so the CE is 74.1% according to Equation (7); (b) Galvanostatic discharge/charge curves of Pt/C//IrO_2-ZAB at 5 mA cm^{-2} for 1.6 h per cycle (0.87 h charge and 0.73 h discharge). Considering m_{Zn} is 0.14591 g, discharge capacity (C_d) is 3.65 mAh, and charge capacity (C_c) is 4.35 mAh, so the CE is 70.1% according to the Equation (7).

Table S1 The area ratios of different Raman peaks for NPC, NPC-Na, NPC-Zn and NPC-Fe.

Samples	**D_2**	**D_1**	**D_3**	**G**
NPC-Fe	25.6%	30.0%	23.9%	20.5%
NPC-Zn	18.2%	35.0%	24.1%	22.7%
NPC-Na	17.6%	39.6%	18.5%	24.3%
NPC	17.5%	27.8%	32.8%	21.9%

Table S2. Atomic ratios of C, N, and O according to XPS results.

Samples	C (at%)	N (at%)	O (at%)
NPC-Fe	95.65	3.44	0.91
NPC-Zn	94.69	3.97	1.34
NPC-Na	94.78	4.01	1.21
NPC	96.25	2.43	1.32

Table S3. sp^3-C/sp^2-C ratio, BET SSA and ECSA of all the samples in this work.

Samples	sp^3-C/sp^2-C	BET SSA (m^2 g^{-1})	ECSA (m^2 g^{-1})
NPC	0.35	161.63	116.2
NPC-Na	0.65	23.26	91.9
NPC-Zn	0.57	1912.29	1249.4
NPC-Fe	0.48	900.80	747.5

Table S4. The proportions of different N-configurations for all the samples in this work calculated from the XPS N 1s results.

Samples	PyN (at%)	PyrN (at%)	GrN (at%)	OxN (at%)
NPC-Fe	19.14	30.22	44.07	6.57
NPC-Zn	32.72	42.28	16.86	8.14
NPC-Na	32.40	39.71	23.63	4.26
NPC	10.62	81.68	5.86	1.84